Proceedings of the 26th International Conference on
Port and Ocean Engineering under Arctic Conditions
June 14-18, 2021, Moscow, Russia

Experimental investigation of viscous-elastic properties of columnar sea ice

Marchenko, A.[1], Karulin, E.[2], Chystiakov, P.[3]
[1]The University Centre in Svalbard, Longyearbyen, Norway
[2]Krylov State Research Centre, St. Petersburg, Russia
[3]Lomonosov Moscow State University, Moscow, Russia

ABSTRACT

Thermally grown sea ice has columnar structure where the porous space is filled by liquid brine and gases. The columnar structure influences anisotropic properties of sea ice. The dependence of ice porosity from the temperature makes these properties temperature and salinity dependent. Under the loading ice demonstrates elastic behavior, creep, stress relaxation and anelastic properties (delayed elasticity). Differences of rheological properties of sea ice in the vertical and horizontal directions are demonstrated by the data of experiments with vertical and horizontal samples (ice cores and beams) of natural sea ice.

KEY WORDS: columnar sea ice, elasticity, viscosity, delayed elasticity.

INTRODUCTION

The use of icebreakers and cargo ships for the delivery of equipment and materials to and from offshore structures located in shallow water regions with stable fast ice is not always optimal. Regular icebreaker operations near the structures will cause systematic ice loads on the structures. Supporting of ice channels over ice season is expensive. Development and support of transport communications to offshore structures by ice roads in winter season could be more reasonable and profitable in regions with sufficiently thick ice. In this case a part of rigging operations should also be performed from and on the floating ice.

Mechanical properties of sea and fresh ice depending on its temperature, structure, and salinity change over ice season. It influences seasonal plan of transport communications and rigging operations. Estimates of bearing capacity of floating ice should consider rheological properties of ice depending on the loading rate and loading duration. Sea ice and fresh ice have elastic and viscous properties. Importance of viscous-elastic rheology of ice for the bearing capacity discussed by Nevel (1976), Betlaos and Lipsett (1979), Sodhi (1998), Bychkovskii, N.N., Gur'anov (2005). Viscous-elastic models of ice were used for the description of ice deformations caused by moving, vibrating or steady loads (Squire et al., 1996; Kosin et al., 2005). Basic equations were derived from the momentum balance of ice sheet using the hypotheses of Kirchhoff setting the dependence of ice particles displacements from the transversal coordinate perpendicular the ice surface, and rheological equations describing the

dependence of stresses from strains (Timoshenko and Woinovsky-Krieger, 1959). Rheological equations introduce the specific of ice properties in mathematical problems.

Anisotropic elastic properties of Ih ice are weak although the ice has hexagonal crystal lattice (Rottger et al, 1994; Schulson and Duval, 2009). It explains a small difference of the elastic constants characterizing elastic behavior of hexagonal ice crystal and small difference of the coefficients of thermal expansion of ice in different directions and gives a possibility to consider fresh ice as isotropic material in physical and engineering problems. Anisotropy of viscous properties of Ih crystals leading to localizing of shear deformations along basal planes is well known (McConnel, J.C., 1891).

Anisotropic structure of columnar sea ice appears at the spatial scale associated with the sizes and shapes of ice grains. It is well known that columnar sea ice consists of vertically extended grains with horizontal C-axes (Weeks, 2010). Liquid brine of sea water is included in the space between ice grains, and brine packets can also exist inside the grains. Difference of sea ice strength in the vertical and horizontal directions was discussed in many papers (Timco and Weeks, 2010). Sea ice strengths in horizontal directions are usually smaller the strengths in vertical direction. Columnar sea ice S_2 can be considered as transversally isotropic material which properties are different in the horizonal and vertical directions. Columnar sea ice S_3 has additional symmetry related to dominant direction of C-axes. Since the orientation of C-axes has small influence on anisotropic properties of fresh ice it is possible to assume that anisotropy of S_3 sea ice is also weak in horizontal directions.

In this paper we compare elastic and viscous properties of columnar sea ice in vertical and horizontal directions. The experiments were performed with samples on natural sea ice taken in the Van Mijen Fjord of Spitsbergen in March 2020. We used acoustic method in combination with vibrating beam tests to calculate dynamic Yong's moduli and Poisson's ratios of vertical and horizontal sea ice samples. Stress relaxation and delayed elasticity effects were investigated by the compression tests with vertical and horizontal ice cores.

DYNAMIC MEASUREMENT OF ELASTIC CONSTANTS

The elastic properties of isotropic materials are characterized by the Young's modulus (E) and the Poisson's ratio (ν). The dynamic values of E and ν are calculated from the measurements of the speed of longitudinal (c_l) and transversal (c_t) waves determined by the formulas (Timoshenko and Goodier, 1951)

$$c_l = \sqrt{\frac{E(1-\nu)}{\rho(1+\nu)(1-2\nu)}},\ c_t = \sqrt{\frac{E}{2\rho(1+\nu)}}, \tag{1}$$

where ρ is the density. Weeks and Assur (1967) noted that accurate determinations of the velocity of propagation of shear waves in sea ice are much rarer than determinations on compressional wave velocities. Therefore, Langleben and Pounder (1963) combined measurements of c_l and resonant frequencies of ice cores to calculate E and ν. Their data are approximated by the formulaы $E = 10 - 0.0351\,\nu_b$ and $\nu = 0.295 \pm 0.009$, where ν_b is the liquid brine content (ppt). Their measurements were performed for $0 < \nu_b < 90$ ppt.

Figure 1 shows the importance of information about ν and ice density (ρ) for the calculation of E when the value of c_l is measured. Ranges of c_l and ρ correspond to measured values of the velocities of longitudinal waves and ice densities (Lin'kov, 1958; Weeks and Assur, 1967).

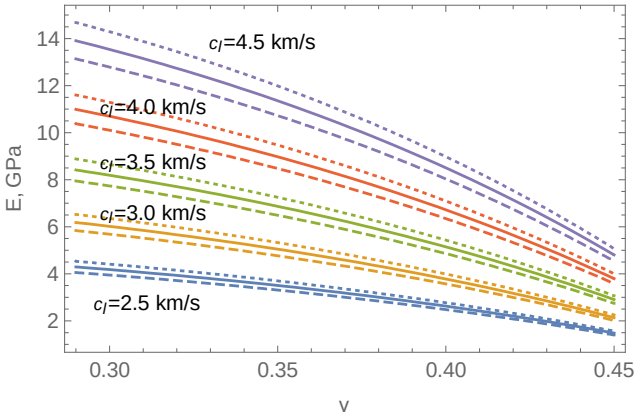

Figure 1. Elastic modulus (E) versus the Poisson's ratio (ν) calculated with different values of the velocity of longitudinal waves (c_l). Ice density (ρ) equals 850 kg/m^3(dashed lines), 900 kg/m^3 (solid lines), and 950 kg/m^3 (dotted lines).

Tabata (1959) measured the natural resonance frequency of sea-ice bars with dimensions of roughly 2x3.5x35cm for the calculation of E. The Poisson's ratio effect on the first natural frequency of a bar is small since there are no stresses at the lateral surfaces of the bar. The first natural frequency of a bar derived in the beam theory depends on the bar sizes and the elastic modulus and doesn't depend on the Poisson's ratio (Landau and Lifshitz, 1986). Further we use this method to calculate E of ice beams. Then, the longitudinal velocity c_l and the density ρ of the ice beams were measured, and the first formula (1) was used to calculate the Poisson's ratio ν.

Vertical and horizontal beams of columnar sea ice were made from sea ice near Kapp Amsterdam in March 2020. The thin sections are shown in Fig. 2. Sea ice was columnar with the horizontal size of columns of 1-3 cm. The ice near Kapp Amsterdam was of S3 type because of the influence of tidal current of alongshore direction. The experiments with vibrating vertical beam were performed in the laboratory in May 2020, the experiments with vibrating horizonal beams were performed in the laboratory in October 2020. The longitudinal velocities were measured in March 2021.

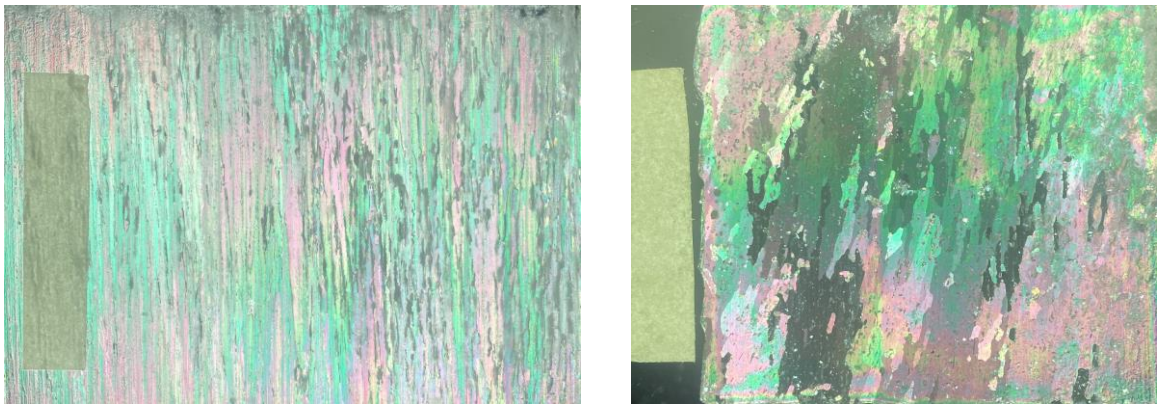

Figure 2. Vertical (left) and horizontal (right) thin sections of sea ice taken near Kapp Amsterdam.

Vibrating beam test is shown in the left panel of Fig. 3. The ice beam is placed on two cylindrical supports. The uniaxial accelerometer Bruel & Kjær DeltaTron Type 8344 designed for the measurements of vibrations in the frequency range from 0.2 Hz to 3 kHz is glued by

silicone lubrication in the middle of the upper surface of the beam. The weight of the accelerometer is 179 g, and its size in the vertical and horizontal direction is of about 3 cm. The accelerometer is connected by a wire to the amplifier SomatXR MX840B-R. The sampling frequency was set to 10 kHz. The beam vibrations are generated by a finger shock on the beam in the vertical direction. The example of the acceleration record and the spectrum of recorded accelerations are shown in Fig. 4.

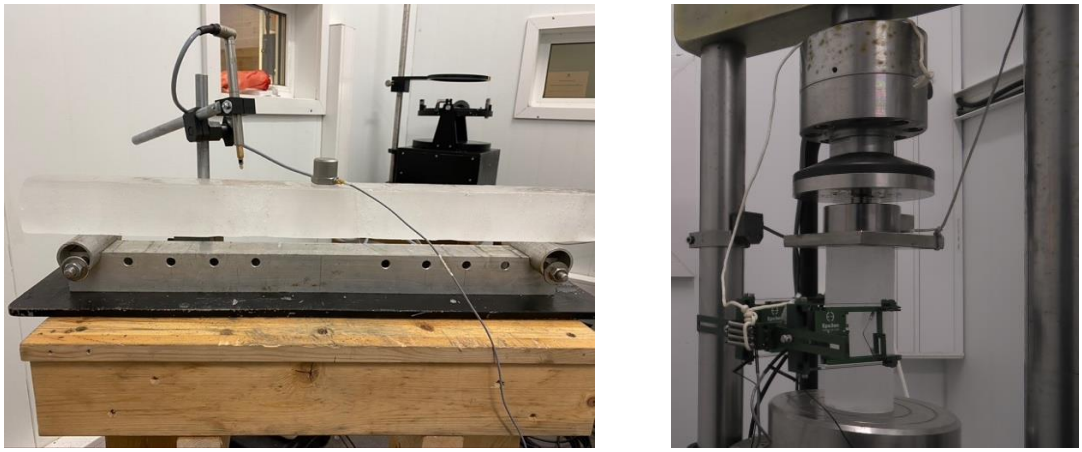

Figure 3. Tests with vibrating beam (left), test with ice core on relaxation and delayed elasticity (right).

Lengths of beams used in the experiments varied from 40 to 70 cm, and their transversal sizes varied within 4-7 cm. For the measurements of ice density ice prisms were made by band saw and milling machine and weighed. The density was calculated by dividing of the prism mass on the volume. Salinity of each beam was measured by melting of beam fragments and measuring of melt water salinity. We recognized a drop of the ice salinity on 2-3 ppt after the delivery and storage of ice samples in the cold room during one month in comparison to the ice salinity measured in the field conditions. After the first month of the storage the salinity of ice samples didn't change significantly with time.

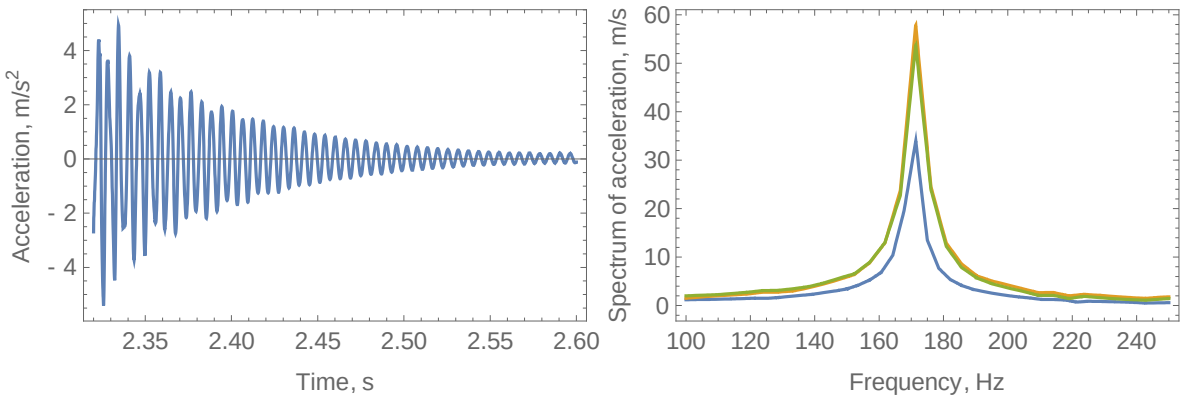

Figure 4. Example of accelerations recorded in the vibrating beam test (left). Spectrum of the recorded accelerations (right).

Comsol Multiphysics Software was used to calculate the natural frequencies of the beams. Measured beam sizes and ice densities were used in the simulations. The value of elastic modulus was adjusted by iterations to get the value of simulated natural frequency similar the

measured frequency in each test. Representative value of the Poisson's ratio 0.33 was used in the simulations since the simulation results have little dependence on the Poisson's ratio.

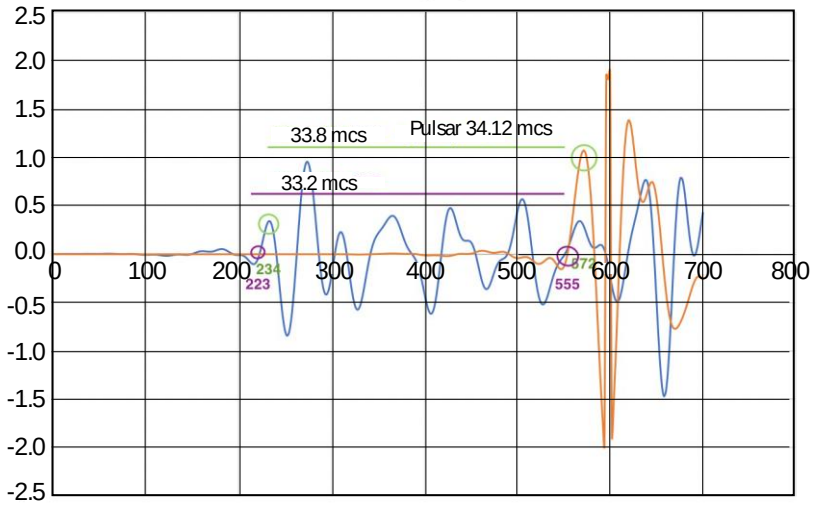

Figure 5. Blue and red lines correspond to the wave forms recorded by Micro-SHM transducers mounted together with Pulsar transducers on the same ice sample.

The speed of longitudinal waves was measured with ultrasonic pulse velocity test instrument Pulsar 2.2 (https://interpribor.com/ultrasonic-testing-of-concrete). Acoustic signals generated by Pulsar with frequencies 60-65 kHz were recorded by acoustic system Micro-SHM (Mistras) equipped with transducers PK15I, 150 kHz with Integral Preamplifier (https://www.physicalacoustics.com/by-product/micro-shm-structural-health-monitoring-system/). The sampling frequency of Micro-SHM was 5 MHz. The transducers PK15I were mounted together with Pulsar transducers on the same sample of fresh ice. The time of signal propagation between the transducers provided by Pulsar was compared with the time between the registrations of wave fronts recorded by Micro-SHM (Fig. 5). The comparison was performed in the temperature range (-20C, -2C), and we found that the times of signal propagation between the Pulsar transducers were similar the times of wave fronts propagation between PK15I transducers of Micro-SHM.

Results of the vibration tests with vertical ice beam are shown in Table 1. All tests were performed with the same beam and different ice temperatures. The beam length was 42 cm. The transversal cross-section of the beam was a square with 5 cm size. The beam was supported at the free ends so that the distance between the points of support was equal to the beam length. The ice density was $\rho = 842$ kg/m^3, and the ice salinity was 3.5 ppt. The longitudinal speed $c_l \approx 3.6$ km/s was measured after the tests.

Table 1. Elastic moduli of sea ice calculated from the vibration tests with the vertical ice beam at different temperatures.

T, C	-19	-12	-10	-5
E, GPa	7.8	8.2	8.5	7.2
ν	0.31	0.29	0.28	0.34

Results of the vibration tests with horizontal ice beams are shown in Table 1. The tests were performed with ice beams of different sizes at the same ice temperature -10 C. The speed c_l, ice density, and ice salinity of each beam were measured after the vibration test. One can see

that elastic moduli is the horizontal direction (Table 2) are smaller the elastic moduli in the vertical direction (Table 1). The Poisson's ratios were calculated larger in the horizontal direction than in the vertical direction.

Table 2. Elastic moduli and Poisson's ratios of sea ice calculated from the vibration tests with horizontal ice beams at -10 C.

	1	2	3	4	5	6	7
ρ, kg/m^3	874	854	864	915	903	945	950
S, ppt	4.65	5.96	2.78	2.75	3.00	2.98	3.01
c_l, km/s	4.3	3.7	4.3	4.4	4.3	4.3	4.3
E, GPa	6.25	3.2	3.5	4.4	7.1	5.4	6.8
ν	0.42	0.45	0.46	0.45	0.41	0.44	0.42

INVESTIGATION OF VISCOUS PROPERTIES OF COLUMNAR SEA ICE

Experiments of the measurement of viscous properties of columnar sea ice were performed with vertical and horizontal cores of sea ice taken from the same place as the ice beams in March 2020. The tests were performed in the cold laboratory of UNIS by the test machine Knekkis. The load was measured by two similar HBM load cells 10 T mounted in the rig and placed on the surface of ice core (right panel in Fig. 3). Records of the second load cell were synchronized with the records of the EpsilonTech extensometer, with 50mm base, mounted in the middle part of the ice core. Records of the Knekkis load cell were synchronized with the records of vertical displacement of the plate supporting the ice core in the rig.

a)  b) 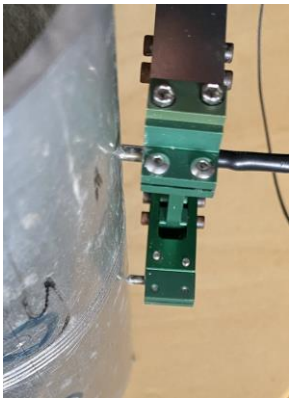

Figure 6. Mounting of EpsilonTech strain sensor on a pipe by 4 pins: top view (a), 2 pins on the side of the pipe.

The loads measured by both load cells were similar in all tests. Deformations recorded by EpsilonTech extensometer were usually smaller the deformations calculated from the records of the displacement sensor in the Knekkis. The difference is explained by ice failure effects at the edges of ice cores. We are sure that strains measured by EpsilonTech sensor reproduces better the strains in the middle part of ice cores which are most important for the description of ice rheology.

Nevertheless, we think that ice strains recorded by EpsilonTech sensor in some tests with fast deformations can be wrong. Figure 6 shows mounting of EpsilonTech sensor on a pipe. The sensor is connected to the pipe by 4 pins compressed to the pipe by a spring. The weight of the sensor (270 g) may cause a sliding of the pins by the surface of ice cores and even its drops. The fall of sensor on the floor was prevented by a security cord. Preventing of the sliding during

fast elastic deformations was problematic. It would be possible to freeze the pins inside small drilling holes, but we decided don't drill the surface of ice cores in 4 places to avoid concentrations of stresses.

Table 3. Densities (kg/m^3) and salinities (ppt) of horizontal (H) and vertical (V) ice cores used in the tests on ice strength (IS), stress relaxation (SR), and delayed elasticity (DE).

T, C	-5		-10		-16		-20	
	H	V	H	V	H	V	H	V
IC	685/3.6	…/4.1	978/4.9	864/4.9	872/3.9	917/4.6	852/4.9	876/4.0
SR	966/4.0	854/4.0	903/4.0	978/5.0	866/5.3	852/4.9	856/3.5	900/4.2
DE	971/2.75	900/…						

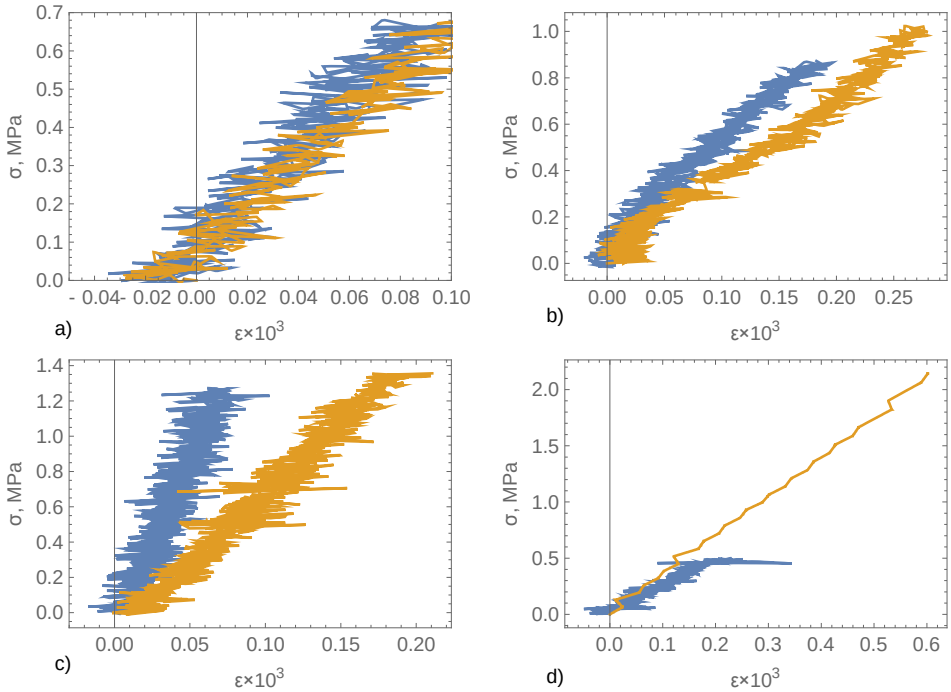

Figure 7. Compressive stress versus deformation from IC tests with horizontal (blue line) and vertical (yellow line) ice cores. The ice temperature is -5ºC (a), -10º C (b), -16ºC (c), and -20ºC (d).

Three types of tests on ice compression (IC), stress relaxation (SR), and delayed elasticity (DE) were performed with the ice temperatures -5C, -10C, -16C and -20C. Densities and salinities of ice cores used in the tests are shown in Table 3. Ice density was calculated by the dividing of ice core weight on ice core volume. Ellipsis in Table 3 means that the weight of the ice core was not measured. IC tests were performed with constant strain rate of 0.001 s^{-1}. Figure 7 shows fragments of stress-strain dependencies of IC tests where they are linear and have maximal slope angles. The strains were measured by the EpsilonTech extensometer. The tangent of the slope angle equals to the effective elastic modulus E_{eff}. The effective elastic moduli found from Fig. 7 are 7 GPa for vertical and horizontal cores at -5ºC, 5.3 GPa for vertical and horizontal cores at -10ºC, 7 GPa for vertical core at -16ºC, 3.3 GPa for vertical core at -20ºC, and 2.8 GPa for horizontal ice core at -20ºC. Blue line in Fig. 7 c shows very high value of E_{eff}. We think that the error is related to bad mounting of the EpsilonTech pins on the ice core surface.

In SR tests the fixed load was applied to the ice cores during 10 min, then the displacement rate of the Knekkis rig was placed to zero, and the load was recorded during another 10 min. The results of SR tests are shown in Fig. 8a (horizontal core) and Fig. 8b (vertical cores). The load was about 50% of the compression strength measured in IC tests. Only in the first test with horizontal ice core at -5°C the load was applied during 190 s (blue line in Fig. 8a). Stress relaxation was observed in all tests, but only in the first test the load dropped to zero after 300 s of the relaxation. Table 4 shows the portion of stresses relaxed during 10 min in comparison to the initial stress in different tests. It is obvious that stress relaxation was stronger in the horizontal ice cores. Relaxation in the horizontal cores is temperature dependent: the portion of stresses relaxed during 10 min decreased with the temperature decrease. This temperature effect was not discovered in the tests with vertical ice cores.

Table 4. Reduction of stresses (%) in SR tests.

T, C	-5	-10	-16	-20
H	100	80	77	70
V	17	21	21	17

In DE tests a fixed load was applied to ice cores during some time and then removed. After the load dropped to zero the deformations of ice cores were recorded by the EpsilonTech extensometer. DE tests were performed with same vertical and horizontal ice cores at -5°C. Figure 9 shows stress and strain versus time in DE tests performed with horizontal and vertical ice cores. The test was repeated 3 times with the same horizontal ice core, and 2 times with the same vertical ice core. Blue, yellow, and green lines correspond to the first, the second and the third tests. Therefore, initial deformations on blue, yellow, and green lines are different in Fig. 9b, d. It is evident that deformations of the horizontal cores were much larger the deformations of the vertical cores despite the loads were almost similar. When the load is removed the vertical cores demonstrated sudden drop of the deformations (Fig. 9d). It can be explained by significant portion of elastic deformations stored in the ice. This effect also may relate to the displacements of the EpsilonTech pins as a reaction on high strain rate of the core. The delayed elasticity effect in the horizontal ice cores is smoother (Fig. 9b).

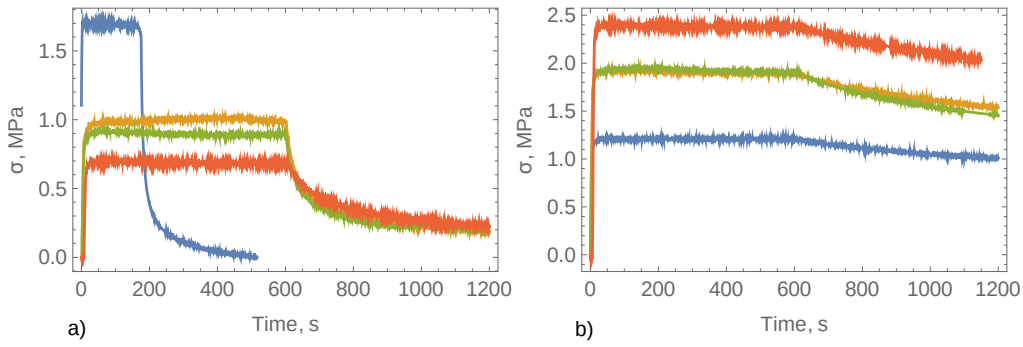

Figure 8. Stress versus time in SR tests performed with horizontal (a) and vertical (b) ice cores. The ice temperature is -5°C (blue lines), -10° C (yellow lines), -16°C (green lines), and -20°C (red lines).

The tangential lines to the strain-time dependencies in Fig. 9b are almost horizontal at t=400 s. It means that the delayed elasticity effect is almost finished at t=400 s in the horizontal ice cores. Figure 9d shows that this effect is extended over t=600 s in the tests with the vertical ice cores. The exponential approximations of anelastic strains (ε_{an}) from the time are shown in Fig. 10 over 300 s. One can see that the strain relaxation time of the vertical cores in twice

bigger compare to the horizontal cores. Red lines in Fig. 10 show exponential approximations of anelastic strains versus time.

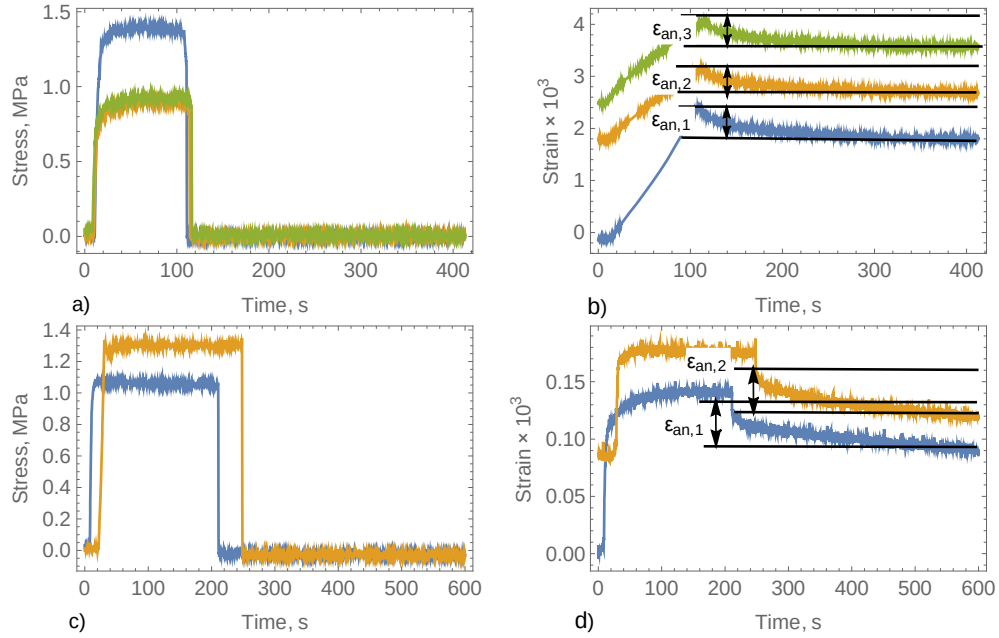

Figure 9. Stress and strain versus time in DE tests performed with horizontal (a,b) and vertical (c,d) ice cores. The ice temperature is -5°C.

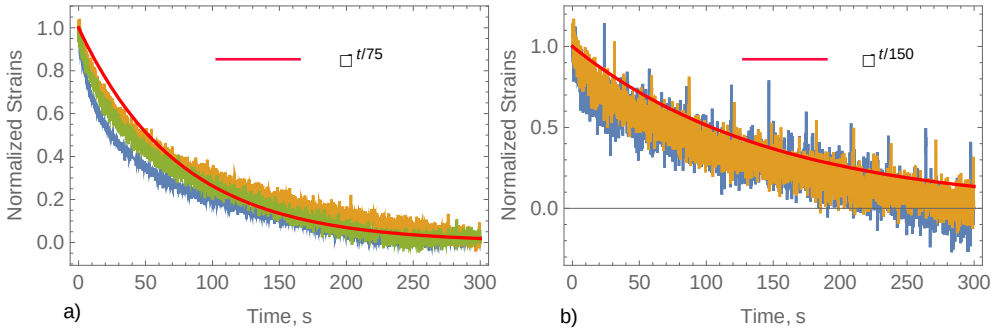

Figure 10. Normalized strain versus time in DE tests performed with horizontal (a) and vertical (b) ice cores. The ice temperature is -5°C.

CONCLUSIONS

Acoustic tests in combination with vibration beam tests were used to calculate the dynamic elastic constants (Young's modulus and Poisson's ratio) of columnar sea ice in vertical and horizontal directions in the temperature range from -20°C to 5°C. I was discovered that the dynamic Young's moduli are larger in vertical directions, and the dynamic Poisson's ratios were larger in the horizontal directions. Stress relaxation tests demonstrated higher rates of stress relaxation in horizontal directions than in vertical direction. Rates of strain relaxation in delayed elasticity tests was also higher in horizontal directions than in vertical direction. Full stress relaxation was measured in the horizontal ice core at -5°C over 300 s. Horizonal ice cores didn't show so fast relaxation at lower temperatures. Vertical ice cores demonstrated mush smaller rates of stress relaxation.

Performed experiments are not enough to formulate rheological model of columnar sea ice as transversally isotropic material with horizontal plane of isotropy. Elastic properties of transversally isotropic materials are described by 5 elastic constants including 4 constants (elastic moduli and Poisson's ratios in vertical and horizontal directions and shear modulus in vertical direction). Method based on the measuring of the speed of longitudinal waves in vertical and horizontal directions and measuring of natural frequency of vibrations of horizontal and vertical ice beams allow to calculate the elastic moduli and the Poisson's ratios. Some additional test should be performed to calculate the shear modulus in vertical direction. We think that it could be a test with vibrating plate sawn from the ice in vertical direction so that normal vector to the plate is in the horizontal plane.

Viscous constants ice can be calculated after the formulation of 3D rheological model of transversally isotropic ice. Rheological constants of isotropic viscous elastic 1D model of ice considered as a Burgers material are calculated from the tests on relaxation, delayed elasticity, and creep (Nowick and Berry, 1972). These tests performed with vertical and horizontal ice samples will give an information for the rheological constants of 3D model. Probably some shear tests should be performed in addition to calculate complete set of rheological constants in 3D model of transversally isotropic ice based on the Burgers rheology. More advanced models describing viscous and anelastic properties of ice were considered by (Cole, 1995; O'Connor et al., 2020). Adaptation of these models for transversally isotropic ice can be not trivial procedure. Investigation of temperature dependence of the rheological constants (Cole, 2020) is important to reproduce the influence of climate changes in the Arctic on ice properties.

Set of rheological constants describing behavior of columnar ice in the horizontal plane is enough for the modeling of bending deformations of ice caused by loads distributed over sufficiently big distances over the ice surface. Typical example is related to ice deformations caused by surface waves. The water pressure in this case takes a role of distributed load. Viscous properties of ice influence wave damping on the way of their propagation below the ice. The rheological constants of ice can be calculated using measurements of wave speed and wave damping (Marchenko et al., 2021). Inversely, measurements of elastic and viscous constants of sea ice in the laboratory tests give possibility to estimate wave damping.

AKNOWLEDGEMENTS

The work was supported by the Research Council of Norway through the IntPart project Arctic Offshore and Coastal Engineering in Changing Climate.

REFERENCES

Beltaos, S. and Lipsett, A. W. (1979) An empirical analysis of the floating ice sheets. Proceedings, *Workshop on the Bearing Capacity of Ice Covers*, pp. 124136. Winnipeg, Manitoba, Canada, National Research Council of Canada, Technical Memorandum No. 123, pp. 124136.

Bychkovskii, N.N., Gur'anov, B.A., 2005. *Ice construction sites, roads, and crossings*. Ministry of Education and Science of Russian Federation, Federal Agency on Education, Saratov State Technical University. (in Russian)

Cole, D.M., 1995. A model for the anelastic straining of saline ice subjected to cyclic loading. *Philosophical Magazine A*, 72(1), 231-248.

Cole, D.M., 2020. On the physical basis for the creep of ice: the high temperature regime. *J. Glaciology*, Vol. 66, 257 , 401 – 414.

Kozin, V.M., Onishchuk, A.B., Mar'in, B.N., Ivanov, Yu. L., Povsyk, N.G., Shport, V.I., 2005. *Icebreaking capacity of flexural-gravity waves from moving vehicles*. Dal'nauka, Vladivostok, 191 p. (in Russian)

Landau, L.D., Lifshitz, E.M., 1986. *Theory of elasticity*. Elsevier Science & Technology, Oxford, United Kingdom, 196 pp.

Langleben, M.,P., Pounder, E.,R., 1963. Elastic parameters of sea ice. In: W.D.Kingery (Editor), *Ice and Snow*, M.I.T. Press, Cambridge, Mass, 69-78.

Lin'kov, E.M., 1958. Study of the elastic properties of an ice cover in the Arctic. *Vestnik Leniagradskogo Universiteta*, 13, 17–22 (in Russian).

Marchenko, A., Haase, A., Jensen, A., Lishman, B., Rabault, J., Evers, K-U., Shortt, M., Thiel, T., 2021. Laboratory Investigations of the Bending Rheology of Floating Saline Ice and Physical Mechanisms of Wave Damping in the HSVA Hamburg Ship Model Basin Ice Tank. *Water*, 13, 1080. https://doi.org/10.3390/w13081080.

Marchenko, A., Karulin, E.B., Chistyakov, P.V., 2020. Experimental studies of inelastic behavior of sea ice. *Vesti gazovoy nauki: Modern approaches and advanced technologies in projects of development of Russian offshore oil-and-gas fields.* Moscow: Gazprom VNIIGAZ, N3 (45), 141-150.

McConnel, J., 1891. On the plasticity of an ice crystal. *Proc. Roy. Soc. (London)*, 49, 323-343.

Nevel D. E., 1976. *Creep theory of a floating ice sheet*. Special Report 764, U.S. Army Cold Regions Research and Engineering Laboratory, Hanover, New Hampshire.

Nowick, A.S., Berry, B.S., 1972. *Anelastic relaxation in crystalline solids*. Academic Press, New York and London, 677.

O'Connor D., West B., Haehnel R., Asenath-Smith E.A., Cole D., 2020. A voscoelastic integral formulation and numerical implementation of an isotropic constitutive model of saline ice. *Cold Regions Science and Technology*, 171, 102983.

Rottger, K., Endriss, A., Ihringer, J., Doyle, S., Kuhs, W.F., 1994. Lattice constants and thermal expansion of H2O and D2O ice Ih between 10 and 265 K. *Acta Crystallographica*, Section B 50, 644–648.

Schulson E.M., Duval P., 2009. *Creep and fracture of ice*. University Press: Cambridge, 401 pp.

Squire V.A., Hosking R.J., Kerr A.D., Langhorne P.J., 1996. *Moving loads on ice plates*. Kluwer Academic Publishers: Dordrecht, 230 pp.

Sodhi D., S., 1998. Vertical penetration of floating ice sheets. *Int. J. Solid Structures*., 35 (31-32), 4275-4294.

Tabata, T., 1959. Studies on mechanical properties of sea ice III. Measurement of elastic modulus by the lateral vibration method. *Low Temperature Science*, A18, 116-129. Translation, American Meterorological Society T - J - 12.

Timco G.W., Weeks W.F., 2010. A review of the engineering properties of sea ice. *Cold Reg. Sci. Techn.*, 60, 107-129.

Timoshenko, S., Goodier, J.N., 1951. *Theory of elasticity*. McGRAW-HILL BOOK COMOPANY, New-York, 506 pp.

Weeks, W., Assur, A., 1967. *The mechanical properties of sea ice*. In Cold Regions Science and Engineering Part II: Physical Science Section C: Physics and Mechanics of Ice. CRREL. DA Project 1VO25001A130.

Weeks, W., 2010. On sea ice. Fairbanks: University of Alaska Press. 664p.